

# Voltage Sensitive Dye Imaging System for Awake and Freely Moving Animals

Joon Hyuk Park<sup>1</sup>, Eugenio Culurciello<sup>1</sup>, Dongsoo Kim<sup>1</sup>,  
Justus Valentijn Verhagen<sup>2</sup>, Shree Hari Gautam<sup>2</sup>, Vincent Pieribone<sup>3</sup>

<sup>1</sup>Department of Electrical Engineering, <sup>2</sup>Department of Neurobiology, <sup>3</sup>Department of Cellular and Molecular Physiology  
Yale University

New Haven, CT 06520

joonhyuk.park, vincent.pieribone, dongsoo.kim, eugenio.culurciello@yale.edu  
jverhagen, sgautam@jbpierce.org

**Abstract**—A 32 x 32 pixel image sensor in bulk CMOS process for use in a custom voltage sensitive dye imaging system is presented. The system is to be mounted on awake and freely moving animals in order to measure brain activity. The image sensor is capable of on-chip temporal-differencing using a storage capacitor on-chip. Temporal-differencing is used to reduce the stress on the overall readout circuitry in order to meet size and power constraints of such a system. Each  $75\ \mu\text{m} \times 75\ \mu\text{m}$  pixel consists of a photodiode of  $74\ \mu\text{m} \times 34\ \mu\text{m}$  and a storage capacitor of 788 fF. The image sensor has a signal-to-noise ratio of 76 dB.

## I. INTRODUCTION

Currently, there are no widely-used methods that allow the optical recording of rapid electrical events over a wide cortical area in freely moving animals. This paper presents a device and method for recording the electrical activity of large regions ( $2\text{-}3\ \text{mm}^2$ ) of the nervous tissue at high speeds ( $> 500\ \text{Hz}$ ) using voltage-sensitive fluorescent dye imaging (VSDI) in awake and freely moving animals.

Neuronal recordings of awake and freely moving animals are desirable because they provide the most representative view of brain function. Experiments using general anesthetic and physical restraints have dramatic effects on all levels of neuronal function [1]. The suppression of activity with anesthetics is especially severe in studies of cerebral cortical activity where anesthetics radically alter and depress neuronal activity. In addition, it is not possible to evoke a majority of trained or natural behaviors in anesthetized animals. Without a conscious behavioral response, it is not possible to study cognitive processing of stimuli. Therefore, the use of awake and behaving animals in neurophysiologic studies are necessary for our understanding of brain function, particularly in cortical sensory systems.

Measuring brain electrical activity using VSDI involves the application of a small fluorescent dye to the brain surface [2]. Once intercalated into the plasma membrane of neurons, the dye molecules alter their fluorescent output in response to changes in the transmembrane voltage. Voltage dye recording does not have a bias for particular neuronal subtypes, can report supra and subthreshold voltage changes in neuronal somata and processes as well as glia. It is becoming increasingly clear that glia networks conduct long range and fairly

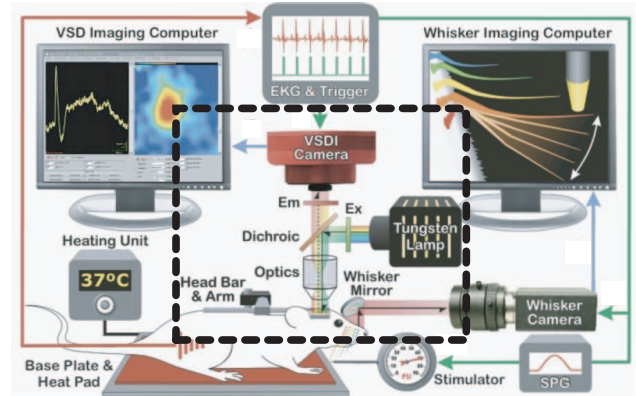


Fig. 1. Current VSDI setup for a fixed, anesthetized rat. The tungsten lamp and the dichroic filter provide the excitation (Ex) signal. The resulting fluorescent signal is passed through the emission (Em) filter and into a image sensor. The stimulator flicks a whisker. The whisker motion is captured with the whisker camera while the motion is compared with the results of the VSDI signal. The proposed system (figure 2) incorporates everything inside the dotted line into a compact system for use on freely moving animals.

rapid calcium and electrical events associated with neuronal activity [3]. VSDI allows the localization of voltage waves as they rapidly propagate across large areas (millimeters) of cortex. Measurements of such widespread rapid electrical events cannot be obtained with electrodes or MRI.

There are other advantages of using VSDI over electrode arrays for observation of rapid electrical activities in the brain. While electrode arrays have proven extremely useful in recording neuronal activity from many neurons ( $< 300$ ) over extended periods of time, this method is limited to recording action potential activity and cannot record subthreshold PSPs, dendritic electrical events, or slow shifts in membrane potential (i.e. up and down states). Also, the signals are very small (a few microvolts) and in many cases, are only 2-3 times the size of noise. Extracellular electrodes are large relative to neurons and their introduction produces damage to significantly more neurons than are targeted for recording [4]. Such damage is concentrated in the first few cortical layers and is therefore not random. Moreover, with time, electrodes loose potency and their signal-to-noise performance significantly declines,

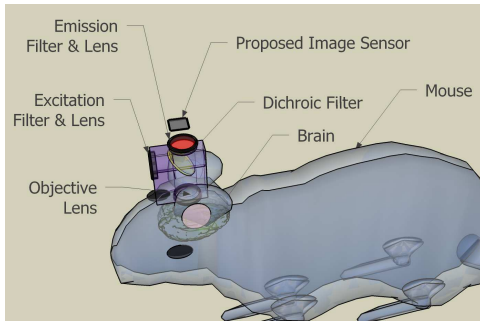


Fig. 2. Proposed VSDI system for freely moving animals. Light from an internal LED passes through an excitation filter, then is reflected by the dichroic filter onto the brain surface. The fluorescent output from brain activities are passed through the dichroic and emission filters onto the image sensor.

due to tissue rejection, gliosis, swelling and retraction [5]. Finally, electrode arrays can only practically record a fraction of neurons in a given area, and do not provide a larger picture of the concerted activity of a brain region.

Wide field VSDI can monitor a far greater area of cortex than is feasible to study with electrodes. The VSDI method can image several square millimeters of cortex simultaneously with no penetrations into the neuropil. In a recent study [6], Ferezou et al. imaged in one field the entire barrel cortex and a portion of motor cortex (over  $20 \text{ mm}^2$ ). It is important to note that high speed (500-100 Hz) wide field optical recordings of electrical activity provide different information about cortical processes that cannot be readily obtained from traditional electrophysiology methods, including propagating sub and suprathreshold waves and state changes, subthreshold events, electrical events in neuron classes inaccessible to electrodes and glial responses [7].

We currently have no system available to make measures of optical signals from wide areas of brain in a freely moving rodent. Typical high-speed VSDI systems use commercial off-the-shelf charge-coupled-devices (CCD) and integrated image sensors that cannot meet the requirements for sensitivity, speed and dynamic-range because of their small pixel sizes and high levels of noise at room temperature [8]. State-of-the-art fluorescent detector arrays for physiological studies are custom, cooled CCD or CMOS cameras mounted on a fixed optical microscope. Such devices are designed for use in fixed large microscopes with anesthetized or restrained animals. Due to size, heat, weight and power limitations, they cannot be adapted for use on freely moving animals.

Figure 2 shows the proposed device for VSDI on awake animals. This paper focuses on the image sensor element of the device. The design requirements for an image sensor for such a device is outlined in Section II. Section III describes the design methodology for the image sensor. The image sensor operation is described in detail in section IV, and the performance of the image sensor is summarized in Section V.

## II. DESIGN REQUIREMENTS

VSDI in an awake and freely moving rodent (rat and possibly mouse) requires a wide field fluorescent voltage imaging of between  $4\text{-}6 \text{ mm}^2$  cortex at high bandwidth (1-2 kHz). VSDI imposes at least three difficulties in the design of a miniaturized implantable sensor. First, the signal-to-noise ratio (SNR) is low, as the signal of interest is around 0.1-1% of the background illumination. Second, one kilohertz bandwidth (1000 frames/s) is needed to sample fast neurophysiologic events [7]. Third, there are a number of dynamic noise sources that together degrade the signal.

VSDI currently requires a specialized illumination source (bright and stable), a high NA image path and a low noise sensor capable of collecting fluorescent images at high speeds [9]. We are producing a custom engineered and manufactured miniaturized head-mounted imaging system that addresses all of these issues.

The imaging system can be of small pixel count, typically  $128 \times 128$  with a large photon-collection area per pixel. Due to the low noise image output, 14-16 bit analog-to-digital converters (ADC) are required. It is important to note that of the 16 bits collected per sample, 10-12 bits are from the unvarying background light. Thus, only 4-6 bits are used to digitize the modulating signal from the tissue.

Weight is a major concern for a head-mounted microscope for small animals. It is not feasible to have multiple 16-bit ADCs on the microscope itself. Putting the ADCs off the system closer to a computer is also undesirable, due to the increase in wires and noise. To address this issue, and to exploit the fact that only 4-6 bits are used to digitize the signal of interest, frame-differencing on chip is implemented. Power and area can be saved because the bright background constitutes 10-12 bits of data, making 16 bit ADCs highly inefficient in our application.

## III. MODELLING OF THE VSDI SIGNAL

The fluorescent light for VSDI has a wavelength of 650 to 700 nm. We used Newport 818-UV calibrated photodiode as a light meter. With either the mini microscope or the macroscope trained on a phantom fluorescent target, the output of the light meter was in the range of 0.4 A to 0.7 A. This fluorescent light corresponds to between  $3 \cdot 10^{12}$  and  $5 \cdot 10^{12}$  photons/s.

Each of our pixels produces 325 pA and 568 pA of current at these intensities. The photodiode capacitance in our design is 788 fF, therefore we obtain a voltage swing in the range of 290 V/s to 507 V/s. Because the fluorescent signal of interest is only a small percentage (0.1-1%) of the whole fluorescent signal, the voltage swing will be in the range of 2.9mV/ms to 5.07mV/ms for a 1% signal of interest.

With the above numbers, and assuming about 1 ms integration time (1000 frames/s), we computed the theoretical upper limit of the signal to noise ratio considering only the shot noise to be approximately 6 bits. This is typical in a VSDI system.

#### IV. IMAGE SENSOR DESCRIPTION

The pixel is shown in Figure 3. The pixel uses a standard 3-T design with a PMOS reset transistor and a NMOS follower. The storage capacitor is a MOSCAP sized for 788 fF. A dummy switch (controlled by  $s1N$ ) is used to reduce clock-feedthrough and charge injection. The pixel value can either be stored into a capacitor and readout through line  $out1$  or can be directly read out using line  $out2$ . Having these two outputs allows the pixel to operate in a normal read-out mode as well as temporal difference mode. For normal read-out, the integrated voltage of the photodiode can be stored into the storage capacitor by turning on  $s1$ . Once integration is finished,  $s1$  is turned off to isolate the storage capacitor from the photodiode. The stored voltage value is then read out.

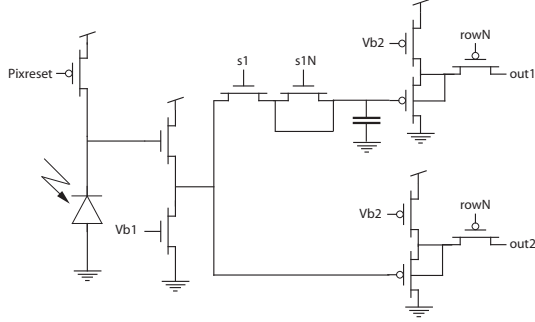


Fig. 3. Pixel used in our image sensor. This pixel is capable of outputting 2 frames sequentially, for temporal differencing on chip.

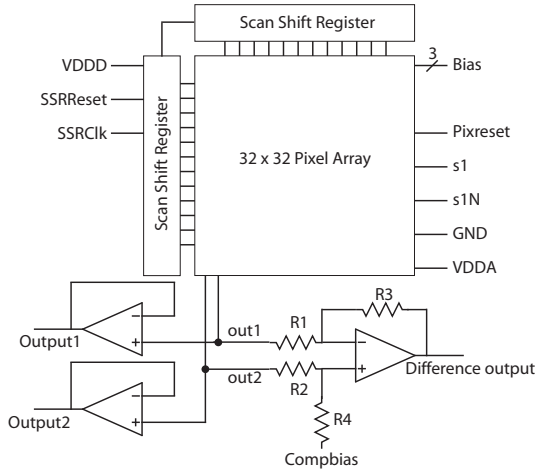


Fig. 4. Complete overview of the image sensor. The shift scan registers are used to address each pixel during readout.  $out1$  and  $out2$  are read by the rest of the system through two buffers. The temporal difference output it generated from the two outputs and read by the rest of the system through *Difference output*. The gain of the differential amplifier is determined by the ratio between  $R1$ ,  $R2$ ,  $R3$  and  $R4$

For temporal difference-mode, the first frame is stored into the capacitor, just as in normal-image mode. However,  $s1$  is turned off after the first frame is integrated and stored. While the storage capacitor is disconnected from the photodiode, the photodiode is reset. Integration starts again for a second

integration time. Then,  $out1$  (containing the previous frame) and  $out2$  (the integrated voltage of the current frame) are read out simultaneously to an on-chip differential amplifier. The differential amplifier has a gain of 8, and allows us to amplify a difference of a few hundred microvolts to a few millivolts. The differential amplifier reduces the number of bits required to discern a 0.1% change from 16-bits to 11 or 12 bits. Figure 4 summarizes the overall image sensor.

Before the integration of a third frame begins, the current values of the photodiode is stored into the capacitor by quickly pulsing  $s1$ . This erases the first frame from the storage capacitor and stores the second frame into the capacitor. This cycle is repeated to produce a continuous temporal-differencing output.

#### V. TESTING AND RESULTS

Various characteristics of the image sensor were tested. First, to test the SNR of the image sensor, the photodiode in every pixel was integrated for 25 ms at different light intensities. As seen in Figure 5, the relationship between SNR (in dB) and light intensity (in lux) are given by the equation:  $SNR = 0.42 \cdot intensity + 31$  before saturation at around 150 lux. The SNR performance determines the fluctuations we can differentiate from the background light and noise. For our application, the SNR needs to be between 55 to 72.

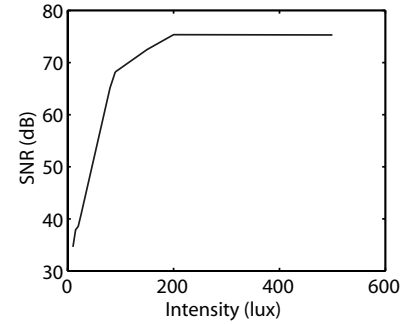


Fig. 5. Signal-to-noise ratio of the image sensor as a function of light intensity at 40 fps.

The leakage of the storage capacitor is needed to determine whether our temporal-differencing will be suitable for this system. If the capacitor loses more than 1/2 of our LSB between frames, we will not be able to accurately measure the signals of interest. In order to test the leakage of the capacitor, the photodiode was reset and  $s1$  was turned off immediately to isolate the capacitor from the photodiode. The voltage drop in the capacitor was measured at different times. The voltage drop in 1 ms is 56  $\mu V$ . For temporal-differencing, value needs to be stored in the capacitor for 2 ms. Even then, there will be a 112  $\mu V$  drop, which is less than 1/2 LSB. Since the storage capacitor is sized to be 788 fF, the leakage current in the capacitor can be calculated to be 44.8 fA.

The fixed pattern noise (FPN) was calculated by measuring the standard deviation of each pixel over 64 frames and then taking the mean of the resulting 1024 standard deviation values. For a short integration time of 20  $\mu s$  in the dark, the standard deviation was 129  $\mu V$  over a 3.1 mV swing. At near

saturation (150 lux and 25 ms integration time), the standard deviation was 308  $\mu\text{V}$  over a 1.298 V swing.



Fig. 6. Sample images from the sensor. Left and center images show the hundredth of a second transition of a stopwatch while the image sensor is running at 700 fps. The right image shows a hand moving in temporal difference mode at 30 fps. The black edges are leading edges and the white edges are trailing edges.

Next, we tested the temporal-difference capability of the image sensor. Figure 6 (right) shows the image sensor detecting the motion of a person's hand. The FPN of the temporal-difference mode was measured using the same method as described above for normal image mode. From 30 to 900 frames/s, the standard deviation of the pixels were in the range of 1.2 mV to 1.6 mV. While the standard deviation may seem high, the output is amplified eight times by the on-chip differential amplifier. Thus, the standard deviation including the comparator noise and the fixed pattern noise, but excluding the gain, is in the range of 150  $\mu\text{V}$  to 200  $\mu\text{V}$ . This is still within our performance requirements.

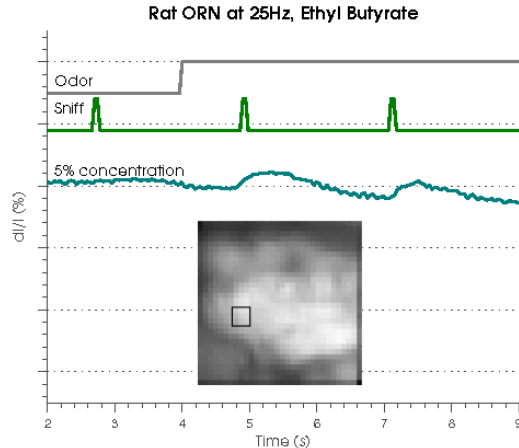


Fig. 7. Calcium dye imaging of olfactory receptor neurons on a live rat using the proposed image sensor. The major ticks of the y-axis are 10% fluctuation of light with respect to the background light.

Finally, the image sensor was placed on a test bench to image olfactory receptor neurons (ORN) in the olfactory bulb (OB) of an anesthetized rat. An odor was delivered to the animal's nose. A double tracheotomy was performed to control sniffing at 2 second intervals with 250 ms sniffing time. The odorant was presented from 4 to 9.5 s. A 2.7% change in background light intensity was detected in glomeruli of the OB once the odor was sniffed. Figure 7 shows the introduction of odor, the sniffing intervals, and the resulting activity detected by the image sensor. The image in the figure shows the field of view (1.5 x 1.5 mm) of the image sensor which was magnified 2x by the optics, and the glomerulus where the activity was detected is outlined with a black box.

TABLE I  
IMAGE SENSOR PROPERTIES

Technology	AMI 0.5- $\mu\text{m}$ Bulk CMOS
Array Size	32 (H) x 32 (V)
Total Size	3 mm x 3 mm
Pixel Size	75 $\mu\text{m}$ x 75 $\mu\text{m}$
Fill Factor	45%
Fixed Pattern Noise	129 $\mu\text{V}$ (dark), 308 $\mu\text{V}$ (150 lux)
Read Noise	67 e-
Output Voltage Swing	1.47 V
Well Size	700,000 e-
Storage Capacitor Leakage Current	44.8 fA
SNR	76 dB
Max Frame Rate	890 fps

## VI. CONCLUSION

The image sensor performs within the requirements for a head-mounted VSDI system for freely moving animals. However, the system will have to be tested on a freely moving animal for verification. There are various aspects of the image sensor that can still be improved for higher performance. Most notably, the speed of the on-chip differential amplifier is the limiting factor in terms of speed. The pixel sizes could also be larger to reduce noise at low light intensities.

## VII. ACKNOWLEDGMENTS

The authors would like to acknowledge the many contributions of Aleksandar Vacic and Wei Tang. This project was partly funded by ONR grant number 439471 and 396490, and ARO contract W911NF-07-1-0597.

## REFERENCES

- [1] T. Berger, A. Borgdorff, S. Crochet, F. Neubauer, S. Lefort, B. Fauvet, I. Ferezou, A. Carleton, H. Lüscher, and C. Petersen, "Combined voltage and calcium epifluorescence imaging in vitro and in vivo reveals sub-threshold and suprathreshold dynamics of mouse barrel cortex," *Journal of Neurophysiology*, vol. 97, pp. 3751–3762, 2007.
- [2] B. Baker, H. Lee, V. Pieribone, L. Cohen, E. Isacoff, T. Knopfel, and E. Kosmidis, "Three fluorescent protein voltage sensors exhibit low plasma membrane expression in mammalian cells," *J Neurosci Methods*, vol. 161, pp. 32–38, 2007.
- [3] K. Buchheim, O. Wessel, H. Siegmund, S. Schuchmann, and H. Meierkord, "Processes and components participating in the generation of intrinsic optical signal changes in vitro," *Eur J Neurosci*, vol. 22, pp. 125–132, 2005.
- [4] R. Biran, D. Martin, and P. Tresco, "Neuronal cell loss accompanies the brain tissue response to chronically implanted silicon microelectrode arrays," *Experimental Neurology*, vol. 195, pp. 115–126, 2005.
- [5] R. Griffith and D. Humphrey, "Long-term gliosis around chronically implanted platinum electrodes in the rhesus macaque motor cortex," *Neuroscience Letters*, vol. 406, pp. 81–86, 2006.
- [6] I. Ferezou, F. Haiss, L. Gentet, R. Aronoff, B. Weber, and C. Petersen, "Spatiotemporal dynamics of cortical sensorimotor integration in behaving mice," *Neuron*, vol. 56, pp. 907–923, 2007.
- [7] M. Zochowski, M. Wachowiak, C. Falk, L. Cohen, Y. Lam, S. Antic, and D. Zecevic, "Imaging membrane potential with voltage-sensitive dyes 198:1-21," *Biol Bull*, vol. 198, pp. 1–21, 2000.
- [8] K. Salama, H. Eltoukhy, A. Hassibi, and A. E. Gamal, "Modeling and simulation of integrated bioluminescence detection platforms," *Biosensors Bioelectron Special Issue Micro Nano Bioeng*, vol. 19, pp. 1377–1386, 2004.
- [9] T.-C. Huang, S. Sorgenfrei, K. L. Shepard, P. Gong, and R. Levicky, "A cmos array sensor for sub-800-ps time-resolved fluorescence detection," pp. 829–832, 2007.